

Article

The Antileishmanial Activity of Eugenol Associated with Lipid Storage Reduction Rather Than Membrane Properties Alterations

Kristelle Hughes ¹, Thanh Binh Le ¹, Patrick Van Der Smissen ², Donatienne Tyteca ², Marie-Paule Mingeot-Leclercq ³ and Joëlle Quetin-Leclercq ^{1,*}

¹ Pharmacognosy Research Group, Louvain Drug Research Institute, Université Catholique de Louvain, Avenue E. Mounier 72, B1.72.03, B-1200 Brussels, Belgium; kristelle.hughes@uclouvain.be (K.H.); binhnt@hup.edu.vn (T.B.L.)

² CELL Unit and PICT Imaging Platform, de Duve Institute, Université Catholique de Louvain, Avenue Hippocrate 75, B1.75.05, B-1200 Brussels, Belgium; patrick.vandersmissen@uclouvain.be (P.V.D.S.); donatienne.tyteca@uclouvain.be (D.T.)

³ Cellular and Molecular Pharmacology Unit (FACM), Louvain Drug Research Institute, Université Catholique de Louvain, Avenue E. Mounier 73, B1.73.05, B-1200 Brussels, Belgium; marie-paule.mingeot@uclouvain.be

* Correspondence: joelle.leclercq@uclouvain.be; Tel.: +32-2-764-72-54

Abstract: Leishmaniasis is a neglected tropical disease that still infects thousands of people per year throughout the world. The occurrence of resistance against major treatments for this disease causes a healthcare burden in low-income countries. Eugenol is a phenylpropanoid that has shown in vitro antileishmanial activity against *Leishmania mexicana mexicana* (*Lmm*) promastigotes with an IC_{50} of 2.72 $\mu\text{g}/\text{mL}$ and a high selectivity index. Its specific mechanism of action has yet to be studied. We prepared large unilamellar vesicles (LUVs), mimicking *Lmm* membranes, and observed that eugenol induced an increase in membrane permeability and a decrease in membrane fluidity at concentrations much higher than IC_{50} . The effect of eugenol was similar to the current therapeutic antibiotic, amphotericin B, although the latter was effective at lower concentrations than eugenol. However, unlike amphotericin B, eugenol also affected the permeability of LUVs without sterol. Its effect on the membrane fluidity of *Lmm* showed that at high concentrations ($\geq 22.5 \times IC_{50}$), eugenol increased membrane fluidity by 20–30%, while no effect was observed at lower concentrations. Furthermore, at concentrations below $10 \times IC_{50}$, a decrease in metabolic activity associated with the maintenance of membrane integrity revealed a leishmaniostatic effect after 24 h of incubation with *Lmm* promastigotes. While acidocalcisomes distribution and abundance revealed by *Trypanosoma brucei* vacuolar H^+ pyrophosphatase (TbVP1) immunolabeling was not modified by eugenol, a dose-dependent decrease of lipid droplets assessed by the Nile Red assay was observed. We hereby demonstrate that the antileishmanial activity of eugenol might not directly involve plasma membrane sterols such as ergosterol, but rather target the lipid storage of *Lmm*.

Keywords: eugenol; *Leishmania*; mode of action; lipid droplets; acidocalcisomes; membrane permeability; membrane fluidity



Citation: Hughes, K.; Le, T.B.; Van Der Smissen, P.; Tyteca, D.; Mingeot-Leclercq, M.-P.; Quetin-Leclercq, J. The Antileishmanial Activity of Eugenol Associated with Lipid Storage Reduction Rather Than Membrane Properties Alterations. *Molecules* **2023**, *28*, 3871. <https://doi.org/10.3390/molecules28093871>

Academic Editor: Manoj K. Pandey

Received: 31 March 2023

Revised: 26 April 2023

Accepted: 29 April 2023

Published: 4 May 2023



Copyright: © 2023 by the authors. Licensee MDPI, Basel, Switzerland. This article is an open access article distributed under the terms and conditions of the Creative Commons Attribution (CC BY) license (<https://creativecommons.org/licenses/by/4.0/>).

1. Introduction

Leishmaniasis is a series of vector-borne diseases, transmitted through the bite of a sandfly infected by *Leishmania* parasites. This disease is endemic to several regions in the world, including some developed countries [1]. In 2020, there were over 208,000 new cases of cutaneous leishmaniasis reported worldwide and nearly 13,000 new visceral leishmaniasis cases [2]. Current therapies include sometimes long, painful, and toxic treatments such as pentavalent antimonial, liposomal amphotericin B, miltefosine, or paromomycin [3]. Furthermore, each therapy is effective for a limited number of *Leishmania* species and, thus, specific forms of the disease.

Liposomal amphotericin B is used to treat visceral leishmaniasis [3]. Its leishmanicidal activity is mediated through the formation of pores in the *L. mexicana* and *L. donovani* promastigote plasma membrane as it binds membrane sterols, namely ergosterol, and cholesterol to a lesser extent [4,5]. Formulations such as Kalsome TM10 were shown to depolarize the mitochondrial membrane, cause ATP levels depletion, and increase reactive oxygen species (ROS) production [6].

Miltefosine is the only oral treatment used against cutaneous leishmaniasis as well as visceral leishmaniasis in endemic regions such as South America and India [7]. The drug is an alkylphosphocholine that has been shown to have several targets in *Leishmania* cells, although its mechanism of action is not fully elucidated [8–11].

In addition to therapy efficacy in specific forms of the disease, only, recent emergence of resistant strains and/or relapses after treatment have been reported for both treatments. For instance, mutations to the enzyme sterol 14 α -demethylase, leading to a decrease in plasma-membrane ergosterol levels [12], and higher levels of multidrug resistance 1 (MDR1), causing greater amphotericin B efflux [13], have been shown to decrease the efficacy of amphotericin B treatments. Many in-laboratory miltefosine-resistant strains obtained through several mutations, lead to drug efflux or a reduction in uptake, and an increase in oxidative stress [14]. However resistant strains have not yet been discovered in clinical isolates against miltefosine, though several relapses after treatment have nonetheless been documented [15,16].

In this context, eugenol could represent a potentially useful molecule. An eugenol oil-in-water emulsion showed beneficial immunomodulatory activity in mice infected with *L. donovani* [17]. Indeed, after 10 days of treatment with the eugenol emulsion, the hepatic and splenic parasites load was significantly decreased compared to untreated infected mice, and the host defense was stimulated as evidenced by an increase in nitric oxide, IFN- γ , and IL-2 levels, a decrease in IL-4 and IL-10 levels, as well as an increase in CD4+ and CD8+ T cells. Nonetheless, the mechanism of action of eugenol on *Leishmania* promastigotes has not yet been elucidated. Previous research conducted in our group showed that eugenol has an antileishmanial activity of 2.72 $\mu\text{g}/\text{mL}$ (16.59 μM) against *Leishmania mexicana mexicana* (*Lmm*) promastigotes, with a selectivity index above 10 against the WI38 human fibroblasts and the J774 macrophage mouse-derived cell line [18].

The aim of the present study was to better characterize the mechanism of action of eugenol on *Leishmania*, other than its immunomodulatory activity. Amphotericin B and miltefosine were used as reference drugs in the different assays, not only to assess the magnitude of the activity but also to better determine underlying mechanisms of action. To this aim, morphological changes to *Lmm* promastigotes after treatment with increasing concentrations of eugenol during 24 h and 72 h were followed by scanning electron and fluorescence microscopy. Membrane permeability was evaluated on liposomes (LUVs mimicking *Lmm* membranes) by following calcein release. Membrane fluidity was studied on both LUVs and *Leishmania* promastigotes by measuring changes in 1,6-diphenyl-1,3,5-hexatriene (DPH) anisotropy. Apoptosis in *Lmm* populations was followed by FACS analysis of the calcein-acetoxymethyl ester (AM)/propidium iodide (PI) dye staining. Metabolic activity through NADH/NAD+ and cytochrome c oxidase was assessed in *Leishmania* by using the Alamar blue assay. Finally, in an effort to elucidate a potential target of eugenol in the metabolism of *Lmm*, the abundance of acidocalcisomes and lipid droplets, respectively, involved in pH and Ca²⁺ homeostasis and energy storage, were quantified in *Lmm* promastigotes using fluorescence microscopy for anti-*Trypanosoma brucei* vacuolar H⁺ pyrophosphatase (TbVP1) and Nile Red labeling.

Altogether, the results show that eugenol possesses a mechanism of action that differs from that of the two known drugs amphotericin B and miltefosine, by targeting lipid storage at concentrations below 10 \times IC₅₀, leading to a stunt in cell growth while maintaining membrane integrity. At concentrations above 25 \times IC₅₀, eugenol causes membrane disruption though without selectively targeting membrane sterols. These data give insight into the mode of action of eugenol to mediate its antiparasitic activity.

2. Results

2.1. Eugenol Induces Round Shape of *Lmm* Promastigotes

To evaluate the general effect of eugenol on *Lmm*, promastigotes were treated for 72 h with 0.01% DMSO (Ctl) or three concentrations of eugenol ($0.5 \times IC_{50}$, IC_{50} , and $2 \times IC_{50}$) or amphotericin B (at IC_{50}). Images were recorded by using scanning electron microscopy (SEM) (Figure 1A).

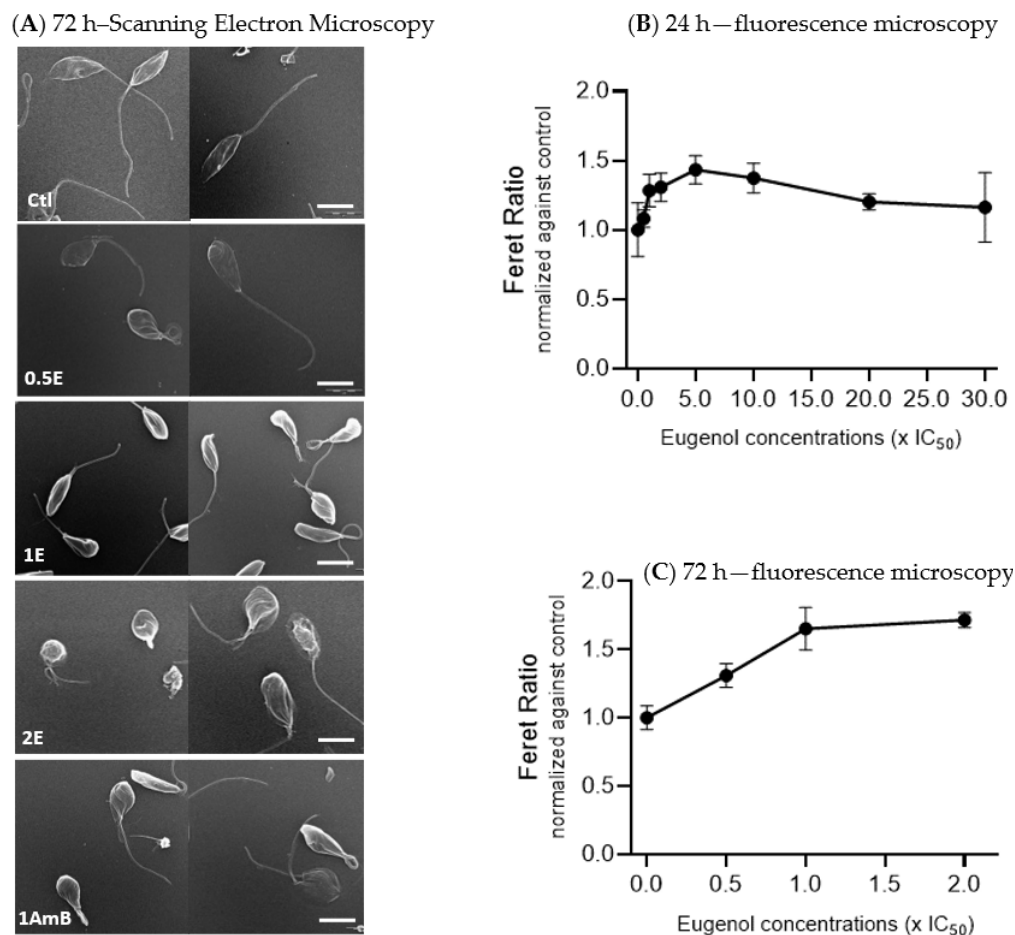


Figure 1. Eugenol induces ultrastructural changes in *Leishmania mexicana mexicana* promastigotes, as revealed by scanning electron and confocal microscopy. (A) Representative images in scanning electron microscopy of *Lmm* treated for 72 h with 0.01% DMSO as control (Ctl), eugenol at 0.5 – $2 \times IC_{50}$ (0.5 – $2E$), and amphotericin B at IC_{50} ($1AmB$). Scale bars, $5 \mu m$. (B,C) Quantification of *Leishmania* morphology by Nile Red labeling in fluorescence microscopy. *Lmm* promastigotes were treated during 24 h (B) and 72 h with eugenol (C). The Feret ratio was calculated from the minimum Feret diameter divided by the maximum Feret diameter. Values \pm SD of 2 independent experiments.

SEM analysis of untreated *Leishmania* promastigotes showed elongated bodies with long flagella. Promastigotes treated with eugenol at $0.5 \times IC_{50}$ appeared more swollen and at IC_{50} and $2 \times IC_{50}$ showed alterations in both shape and size, as observed with gradually rounding promastigote bodies and loss or shortening of their flagella. At $2 \times IC_{50}$, folds appeared on the body of the *Lmm* and their flagella became stumpy. Amphotericin B, at IC_{50} , also showed more round-shaped bodies compared to the control.

Feret ratio values, which describe the shape of the promastigotes (the higher the value, the rounder the object), were calculated. Data revealed an increase of 1.4 fold, reached between 5 and $10 \times IC_{50}$ of eugenol, followed by a decrease back to values comparable to the control at 20 and $30 \times IC_{50}$ of eugenol after 24 h of treatment (Figure 1B). After 72 h of

treatment, a dose-dependent increase of the Feret ratio was observed till 1.7 fold at $2 \times IC_{50}$ (Figure 1C).

Altogether, these results indicate that eugenol induced rounding of *Lmm* promastigotes bodies, similar to amphotericin B.

2.2. Eugenol Induces Milder Membrane Permeability in LUVs Than Amphotericin B

To then evaluate the potential effect of eugenol on membranes, we examined changes in the permeability of large unilamellar vesicles (LUVs) mimicking *Lmm* membranes. Three LUVs compositions were tested. All were composed of phosphatidylcholine (PC), phosphatidylethanolamine (PE), and phosphatidylinositol (PI) but differential sterol content: PC:PE:PI, PC:PE:PI:Cholesterol, or PC:PE:PI:Ergosterol. Each model was treated with increasing concentrations of eugenol and amphotericin B and the calcein leakage was followed (Figure 2).

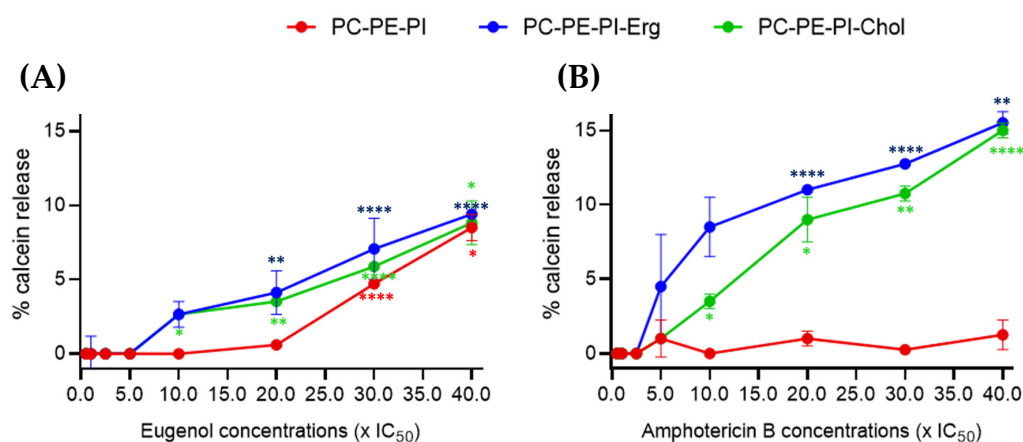


Figure 2. The release of calcein induced by eugenol is lower than that of amphotericin B with differences in sterol dependency. Three LUVs, without sterol (PC:PE:PI; red), with ergosterol (PC:PE:PI:Erg; blue), and with cholesterol (PC:PE:PI:Chol; green), were incubated with increasing concentrations (0.5 – $40 \times IC_{50}$) of eugenol (A) or amphotericin B (B) during 15 min. Fluorescence was measured to follow calcein release and data were expressed in % of calcein release with 0.1% Triton X100, which induces 100% leakage. The values \pm SD were obtained in triplicates for three independent experiments. One-way ANOVA with Dunnett's post tests were performed to compare control versus compound-treated LUVs, * $p < 0.05$, ** $p < 0.01$, *** $p < 0.0001$.

Between 0.5 and $5 \times IC_{50}$, eugenol showed no effect on LUVs, regardless of the liposome composition. At $10 \times IC_{50}$, a low calcein leakage of 2.7% was observed in ergosterol- and cholesterol-containing LUVs. At $30 \times IC_{50}$, a calcein release of 4.7% was observed in sterol-free LUVs. At $40 \times IC_{50}$, ~9% of calcein was released for all three liposome membrane compositions (Figure 2A).

Amphotericin B was used as a reference drug since its interactions with ergosterol in *Lmm* plasma membranes are well known [4,19,20]. No effect was observed until $2.5 \times IC_{50}$. A ~4% calcein leakage was observed starting from $5 \times IC_{50}$ for ergosterol-containing LUVs and from $10 \times IC_{50}$ for cholesterol-containing LUVs, while, as expected, no leakage was observed for the LUVs without sterol even at the highest-tested concentration. A gradual increase was observed for both sterol-containing compositions until $40 \times IC_{50}$ (Figure 2B).

All in all, these data show that eugenol increased LUV permeability at two-times-higher IC_{50} concentrations than amphotericin B. Furthermore, there was seemingly a slight difference in effect between sterol- and nonsterol-containing LUVs treated with eugenol, though no difference between ergosterol- and cholesterol-containing LUVs, suggesting a different mechanism of action than amphotericin B.

2.3. Eugenol Similarly Decreases Membrane Fluidity in Cholesterol and Ergosterol LUVs

Then, using the same eugenol and amphotericin B concentrations as in the permeability assay, we evaluated the membrane fluidity through the measurement of DPH anisotropy. An increase in DPH anisotropy indicates a decrease in membrane fluidity [21]. Only the models containing sterols were kept as there was no significant effect on permeability after treatment in the sterol-free model for amphotericin B.

Between 0.5 and $20 \times IC_{50}$, eugenol showed no significant effect on DPH anisotropy compared to the control. However, starting from $30 \times IC_{50}$, eugenol induced a 30 to 35% dose-dependent decrease in membrane fluidity in both ergosterol- and cholesterol-containing LUVs (Figure 3A).

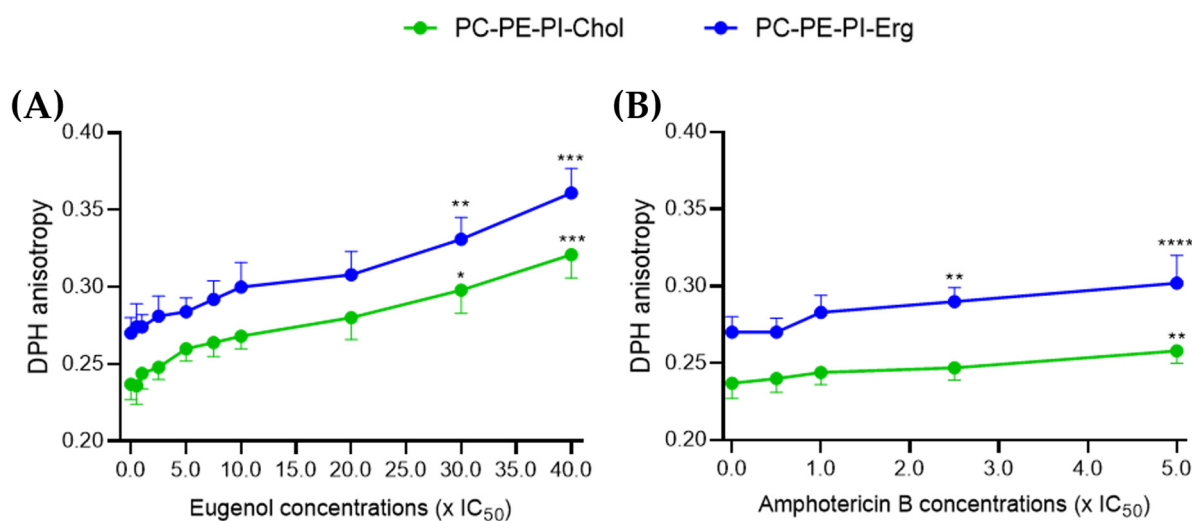


Figure 3. Eugenol similarly decreases membrane fluidity of ergosterol- and cholesterol-containing LUVs. PC:PE:PI:Erg (blue) and PC:PE:PI:Chol (green) LUVs were mixed with DPH at a molar ratio of 1:200 (DPH:lipid) and were incubated for 30 min in the dark with 0.01% DMSO as control, and increasing concentrations of eugenol between 0.5– $40 \times IC_{50}$ (A) and of amphotericin B between 0.5– $5 \times IC_{50}$ (B). Fluorescence was measured to determine DPH anisotropy. The curves represent values \pm SD obtained for triplicates from three independent experiments. One-way ANOVA with Dunnett's post tests were performed to compare the control versus the compound-treated LUVs, * $p < 0.05$, ** $p < 0.01$, *** $p < 0.001$, and **** $p < 0.0001$.

A significant 7% decrease in membrane fluidity was observed after treatment with amphotericin B at $2.5 \times IC_{50}$ and 12% at $5 \times IC_{50}$ in ergosterol-containing LUVs. This is in agreement with previous results that a colloidal suspension containing 45% amphotericin B was shown to decrease the plasma membrane fluidity of *L. amazonensis* promastigotes by increasing EPR spin labeling in a dose-dependent manner [22]. For cholesterol-containing LUVs, only a 9% decrease in fluidity was observed at $5 \times IC_{50}$ (Figure 3B).

Altogether, these results on LUVs indicate that, like amphotericin B, eugenol was able to decrease the membrane fluidity, whether in the presence of ergosterol or cholesterol. However, concentrations of eugenol 15 times higher than those used for amphotericin B are required to show a significant decrease in membrane fluidity.

2.4. Eugenol Increases the Fluidity of *Lmm* Membranes at Higher Concentrations Than Amphotericin B

To enhance the biological relevance of our results and ensure that the differences only in concentrations but not in activity between eugenol and amphotericin B did not result from the simple composition of LUVs, we directly measured DPH anisotropy on the *Lmm* membranes [23,24].

For eugenol, no significant effect was observed below $20 \times IC_{50}$. Between 22.5 and $40 \times IC_{50}$, eugenol increased membrane fluidity by 20–30%, which is contrary to its activity

in LUVs (Figure 4A). Amphotericin B also displayed an increase in membrane fluidity below $3 \times IC_{50}$, while the DPH value increased dose dependently from 0.5 to $5 \times IC_{50}$ (Figure 4B). In contrast, miltefosine showed no significant effect on membrane DPH at any of the concentrations tested (Figure 4C).

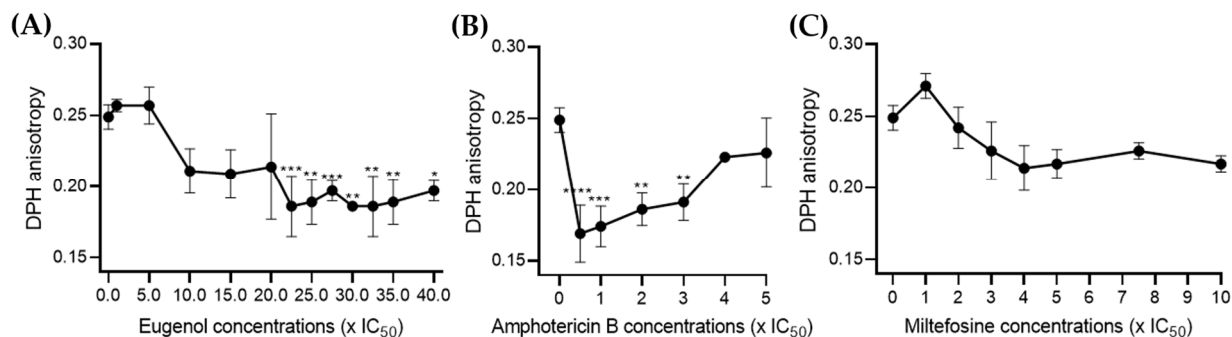


Figure 4. Eugenol increases the fluidity of *Lmm* membranes at concentrations strongly higher than amphotericin B while miltefosine shows no effect. *Lmm* promastigotes at a density of 10^7 cells/mL were treated for 24 h with 0.1% DMSO as control, eugenol at 0.5 – $40 \times IC_{50}$ (A), or amphotericin B at 0.5 – $5 \times IC_{50}$ (B), or miltefosine at 1 – $10 \times IC_{50}$ (C). Fluorescence was measured to determine DPH anisotropy. The curves represent values \pm SD obtained for triplicates from three independent experiments. Significance levels were determined by one-way ANOVA followed Dunnett's post tests to compare control versus compound-treated plasma membranes * $p < 0.05$, ** $p < 0.01$, *** $p < 0.001$, and **** $p < 0.0001$.

In sum, the above data indicate that eugenol induced similar changes to membrane permeability and fluidity than amphotericin B, though alterations were seen at higher concentrations and were less sterol-dependent, which could suggest a different mechanism of action.

2.5. Eugenol Exerts Its Leishmanicidal Effect with Kinetic and Cell-Death Mechanisms Different from Those of Amphotericin B and Miltefosine

To further assess the mode of action of eugenol, we studied the cell-death mechanisms induced by this compound in comparison with amphotericin B and miltefosine.

Calcein-acetoxymethyl ester (AM)/propidium iodide (PI) double labelling can be used on *Leishmania* to distinguish between living, early apoptotic, late apoptotic, and necrotic cells. Contrary to mammalian cells, calcein-AM has greater difficulty entering into viable *Leishmania* cells with intact membranes, resulting in low-to-no fluorescence (calcein−/PI−) [25,26]. During apoptosis, calcein-AM enters the cells where it is cleaved by esterases into a fluorescent molecule. However, at the early apoptosis stage, membrane modifications with the maintenance of the membrane integrity allow calcein-AM entry but prevent PI entry (calcein+/PI−). During late apoptosis, membrane degradation creates pores in the plasma membrane allowing PI to enter the cells (calcein+/PI+). Finally, in necrotic cells, complete membrane loss leads to PI being solely observed (calcein−/PI+) [25].

In Figure 5, between 1 and $15 \times IC_{50}$, eugenol did not induce apoptosis whether the treatment lasted 8 h, 16 h, or 24 h. Only 3.5% of cells were in the late apoptotic stage at 5 and $10 \times IC_{50}$, after 8 h of treatment. At 30 and $32.5 \times IC_{50}$, 9.7% and 16.7% of promastigotes were in early apoptosis, respectively, after 8 h of treatment. After 16 h of treatment at these concentrations, over 95% of cells were necrotic, while after 24 h of treatment, the living cell population rose to 35%, with ~5% early and late apoptotic cells combined. The lower percentage of necrotic cells after 24 h of treatment compared to living cells could be due to more cells evolving from a necrotic state to being completely deteriorated, and thus not detected using our double labeling. Alternatively, the *Lmm* doubling time enabled more

living cells to multiply, increasing their proportion, or cells started adjusting to the presence of eugenol, which led to more cells in the early apoptotic phase than in the necrotic phase.

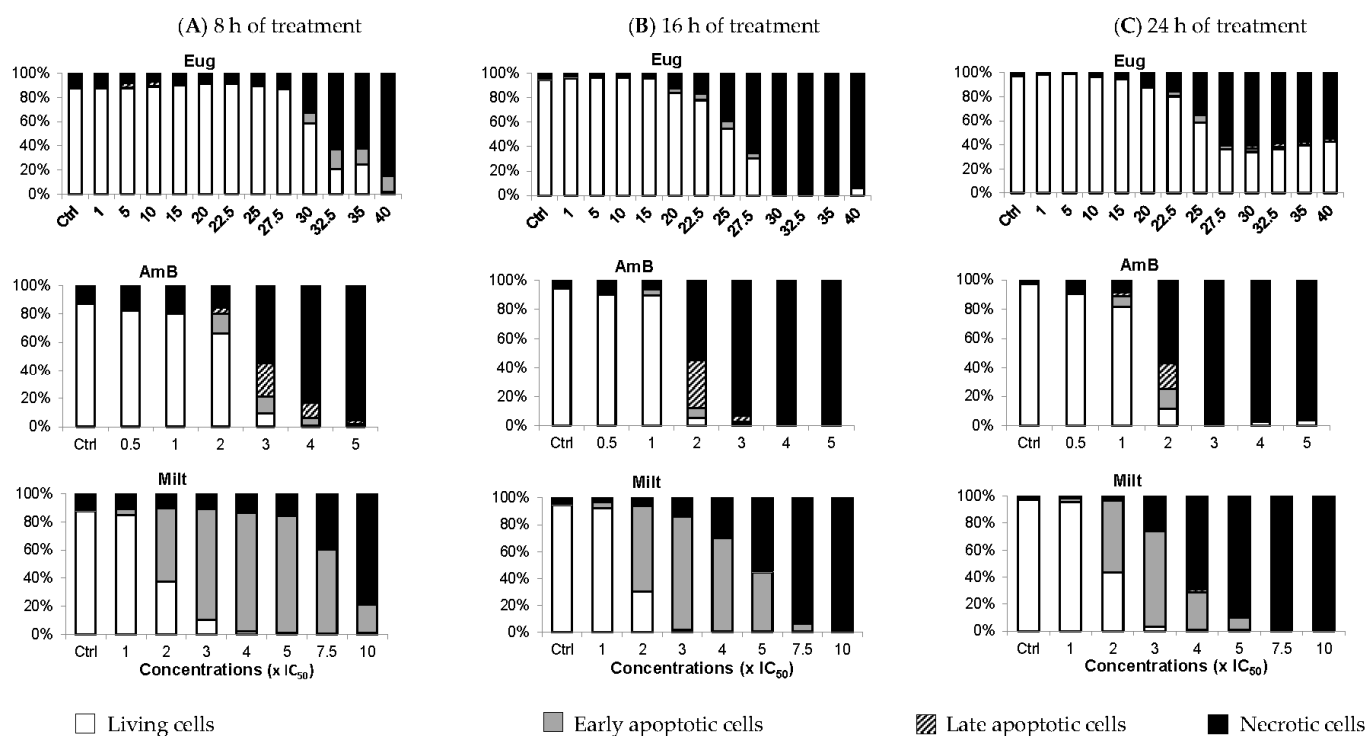


Figure 5. In contrast to miltefosine (Milt) which mainly induces apoptosis, eugenol (Eug) mainly provokes necrosis of *Lmm* promastigotes as amphotericin B (AmB) but at higher concentrations. Percentage of living (white), early apoptotic (grey), late apoptotic (striped), and necrotic (black) *Lmm* promastigote cells obtained after treatment for 8 h (A), 16 h (B), and 24 h (C) by Eug (1–40 × IC₅₀) and by AmB (0.5–5 × IC₅₀), and Milt (1–10 × IC₅₀). Treated cells were labeled with calcein-AM at 0.1 μM and PI at 3 μM, then incubated for 15 min at room temperature in the dark. Green and red fluorescence emissions were measured for calcein and propidium iodide, respectively, by flow cytometry using a 488 nm excitation. The histogram values are the mean of three independent experiments.

In contrast to eugenol, amphotericin B induced early and late apoptotic cells starting at 1 or 2 × IC₅₀ according to the duration of treatment. However, it mainly caused necrosis at higher concentrations. Miltefosine was also added as it was already shown to induce apoptosis in *L. tropica* at 10 μM and *L. major* promastigotes at 22 μM after 18 h, 24 h, and 36 h of incubation by flow-cytometry analysis of annexin V [27]. In the case of miltefosine, *Lmm* cells were in their early apoptosis phase starting at 2 × IC₅₀ for all three treatment durations. Regarding necrosis, the concentration of miltefosine required to induce at least 40% of necrotic cells is inversely proportional to the incubation time.

In conclusion, eugenol induced apoptosis when applied for 8 h at a high concentration (≥30 × IC₅₀). After 24 h of treatment at these concentrations, eugenol likely induced necrosis, a phenomenon that can be linked to membrane disruption via increased membrane permeability and fluidity. At lower concentrations of eugenol, cells were mainly living and membrane integrity was maintained. We, therefore, focused on evaluating the effect of eugenol on metabolic activity to characterize intracellular events that could be responsible for the antileishmanial activity of the compound.

2.6. Eugenol Drastically Reduces Metabolic Activity at Low Concentrations While Maintaining a High Percentage of Living Cells

Alamar Blue is a reagent containing resazurin, a blue dye. Resazurin enters the cell where it is reduced to the highly fluorescent pink-molecule resofurin by enzymes and cofactors such as NADH oxidoreductase or cytochrome *c* oxidase [28–30] without impairing

mitochondrial respiration. It is used to follow cell viability and metabolic function [31], as it is sensitive to changes in energy or respiratory metabolism [32,33]. Furthermore, NADH/NAD⁺ balance and related enzymes have been shown to be crucial in *Leishmania* survival [34]. The metabolic activity data obtained by the Alamar Blue assay were then plotted in comparison with the percentage of living cells obtained by FACS (see Figure 5).

After 24 h of treatment at $10\times IC_{50}$, eugenol reduced the metabolic activity by more than half while simultaneously inducing a 40% loss of *Lmm* division. In contrast, the calcein-AM/PI double labeling showed 95% living parasites at this concentration. The percentage of living cells was reduced by half only at concentrations higher than $25\times IC_{50}$ and reached a plateau at $27.5\times IC_{50}$ (Figure 6A). Amphotericin B and miltefosine both induced a sharp decline in the living-cell population coupled with a dose-dependent reduction of cell growth and metabolic activity (Figure 6B,C).

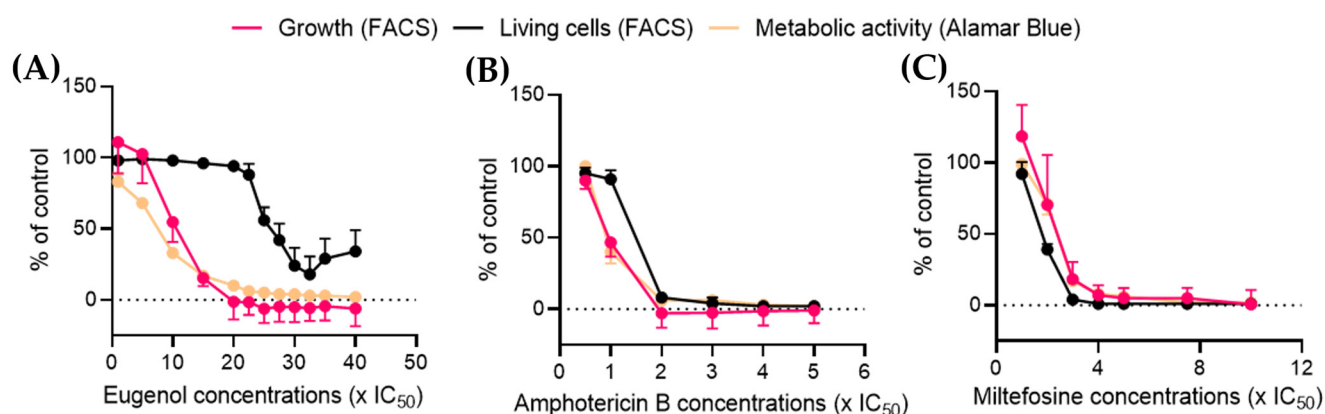


Figure 6. Eugenol reduces the metabolic activity of *Leishmania* while maintaining a high proportion of living cells in contrast to amphotericin B and miltefosine. Metabolic activity was determined with the Alamar blue assay and cell growth was determined by FACS analysis after 24 h of treatment with eugenol at $0.5\text{--}40\times IC_{50}$ (A), amphotericin B at $0.5\text{--}5\times IC_{50}$ (B), and miltefosine at $0.5\text{--}10\times IC_{50}$ (C). The percentage of living cells was obtained from the FACS experiment described in Figure 5. Values are presented \pm SD and were obtained from three independent experiments.

These results indicate that contrary to amphotericin B and miltefosine, eugenol induces a leishmanostatic effect at concentrations below $15\times IC_{50}$, which is characterized by a reduction of metabolic activity and cell growth while maintaining living cell populations.

2.7. Eugenol Reduces Lipid Inclusions but Does Not Impair Acidocalcisomes

Since the metabolic activity of *Lmm* measured by the Alamar Blue assay was reduced in the presence of eugenol, we evaluated whether this observation could be linked to an alteration of polyphosphate storage and osmoregulation in acidocalcisomes and/or lipid metabolism via lipid droplets [35,36]. Acidocalcisomes and lipid droplets were therefore assessed after 24 h of treatment with increasing concentrations of eugenol by fluorescence microscopy upon anti-TbVP1 and Nile Red labeling, respectively.

In Figure 7A,B, no obvious effect on acidocalcisomes was noticed after 24 h or 72 h. This suggests that the overall content and number of acidocalcisomes was not impacted by eugenol.

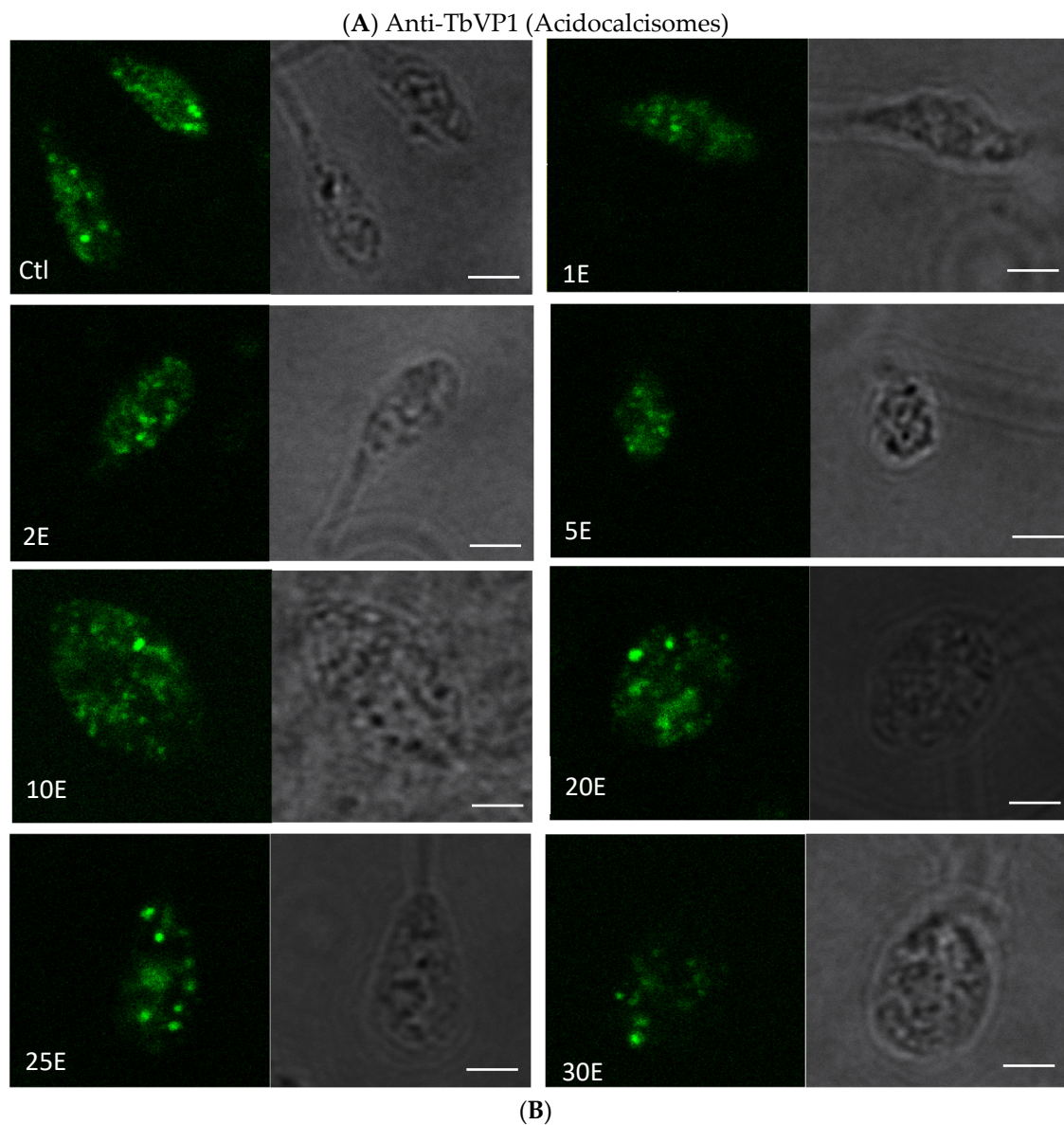


Figure 7. Eugenol does not alter the distribution and abundance of acidocalcisomes, as evidenced by immunolabelling of the vacuolar-type H⁺ pyrophosphatase TbVP1. **(A)** Representative images of acidocalcisomes localization and abundance by anti-TbVP1 immunofluorescence microscopy of *Lmm* promastigotes treated for 24 h with 0.01% DMSO as control (Ctl) and eugenol at 1–30 × IC₅₀ (1–30E) on the left panel and corresponding brightfield images in right panel. Scale bars, 2 μm. **(B)** Image quantification. Values are presented ± SD and are from one experiment with 4–6 images per condition.

In contrast, lipid droplets decreased significantly and dose dependently between $0.5 \times IC_{50}$ and $2-5 \times IC_{50}$, nearly eightfold compared to the untreated promastigotes, before re-increasing (Figure 8A,B).

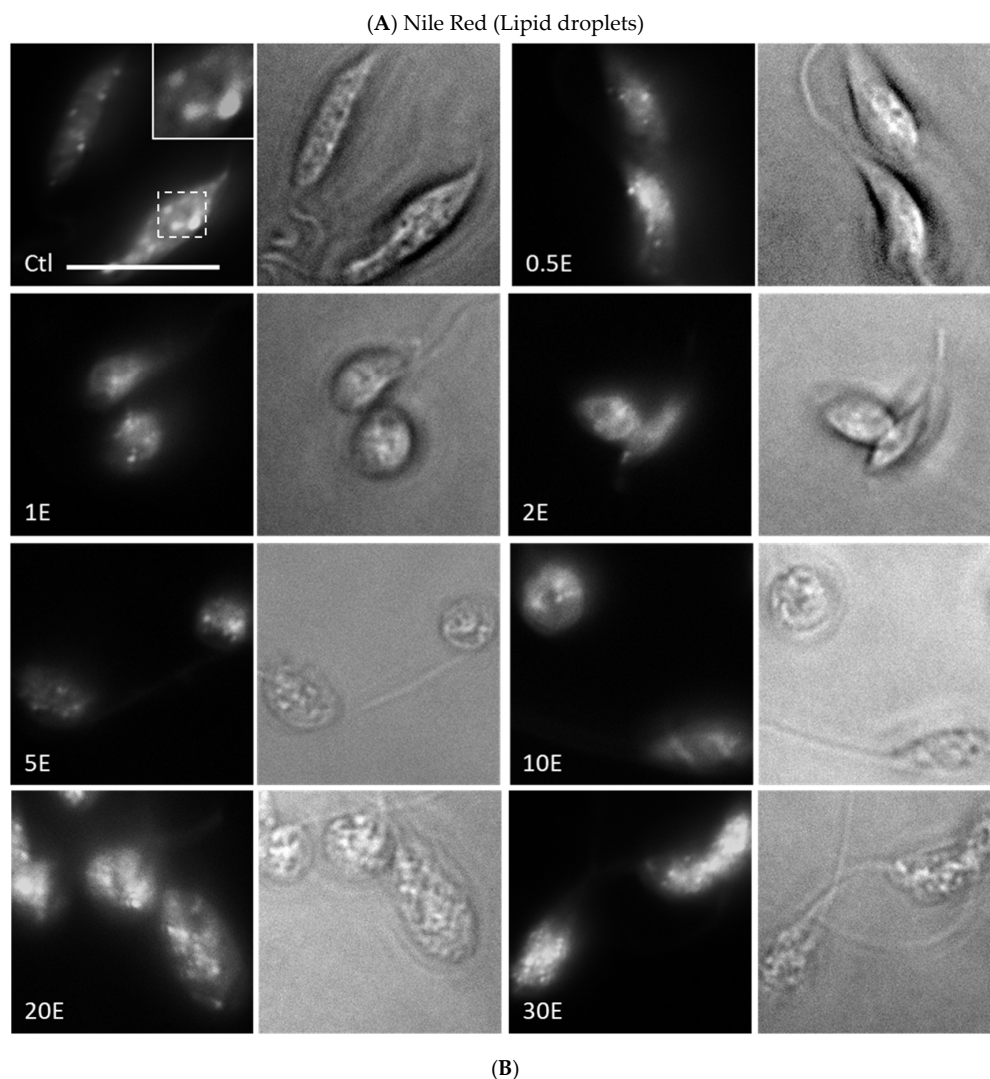


Figure 8. Eugenol decreases lipid droplet labeling, assessed by Nile Red dye. (A) Representative images of lipid droplets by Nile Red fluorescence microscopy of *Lmm* treated for 24 h with 0.01% DMSO as control (Ctl) and eugenol at $0.5-30 \times IC_{50}$ ($0.5-30E$) on the left panel and corresponding brightfield image in right panel. Scale bars, $10 \mu m$. (B) Image quantification. Values are presented $\pm SD$ and represent the average of two independent experiments with 4 to 6 images per condition.

3. Discussion

The effect of eugenol on *Lmm* promastigotes was studied to gain a better understanding of its mode of action. Eugenol-induced rounding of promastigotes after 24 and 72 h of treatment at concentrations around IC_{50} . An increase in membrane permeability and a decrease in fluidity in LUVs were observed at concentrations above $20 \times IC_{50}$, while an increase in the fluidity of *Lmm* membranes was observed at the same concentrations. The results showed that eugenol mainly induced necrosis rather than apoptosis (whether early or late) as a cell-death mechanism, at the various concentrations and incubation periods tested. Further investigation revealed that according to the Alamar Blue assay, metabolic activity related to NADH/NAD⁺ and cytochrome C oxidase was drastically reduced starting at $5 \times IC_{50}$. Lipid droplets were also reduced between 0.5 – $5 \times IC_{50}$ of eugenol while the abundance of acidocalcisomes was not affected. Throughout our experiments, we chose to test eugenol at increasing concentrations up to the ones allowing for a significant effect on the activities studied, while amphotericin B was tested at lower concentrations for which it was already known to have a significant effect. This allowed for the measurement of the difference in the extent and efficacy of eugenol compared to known reference drugs.

The change in promastigotes morphology from elongated to round and swollen was previously observed in the shape of *L. donovani* promastigotes after treatment with a eugenol-rich *Syzygium aromaticum* oil at 100 µg/mL and eugenol emulsions [17,37] as well as several other antileishmanial compounds.

Feret ratios obtained after eugenol treatment of *Lmm* indicate a reduction of body length, describing the shift from elongated to rounded promastigotes. Although the morphology was affected by concentrations near the IC_{50} of eugenol, membrane disruption was neither the cause nor the end result at these concentrations. Eugenol only showed a 10% increase in LUVs permeability at concentrations above $30 \times IC_{50}$. These observations concur with those of a previous publication showing that, at a MIC concentration (or $100 \times Lmm IC_{50}$), eugenol was found to induce 12.5% leakage in *Saccharomyces cerevisiae* membrane-like LUVs [38]. LUVs composition differs between *S. cerevisiae* and *Lmm* models, though, in both cases, weak LUV membrane permeability was observed at high concentrations ($>20 \times IC_{50}$). Nonetheless, amphotericin B is known to target *Lmm* membranes and showed a comparable increase in the permeability to eugenol, although at concentrations approximately 30 times lower than eugenol ($0.25 \times IC_{50}$ instead of $7.5 \times IC_{50}$). This indicates that, although the permeabilizing effect is present with high doses of eugenol, the extent of the disruption might be comparable to that of amphotericin B. Furthermore, a closer investigation of the impact of eugenol on the membranes highlighted a different mode of action than that of amphotericin B. Indeed, the activity of eugenol does not appear dependent on the presence of sterols (ergosterol or cholesterol) in LUVs, while amphotericin B is known (and shown) to preferentially target ergosterol-containing LUVs [19].

Similar to permeability, membrane fluidity is only significantly affected by eugenol at concentrations above $20 \times IC_{50}$. In this regard, loss of membrane integrity mainly occurs at high concentrations of the compound and leads to necrosis. The high concentrations needed to observe membrane disruption suggest the role of other membrane components than the lipids included in the LUVs. Furthermore, the opposite effects on the membrane fluidity of LUVs versus *Lmm* membranes were observed. This could be due to differences in the components present in artificial membranes and membranes from parasites, and especially the presence of membrane proteins. Furthermore, differences in experimental conditions such as the duration of incubation (30 min for LUVs experiments and 24 h for *Lmm* plasma membranes) could also explain the differences in results since the compounds could be differently inserted in the membrane because of a lesser or greater duration of contact with the membranes, thus modifying the DPH location [39].

Intracellularly, nuclear DNA fragmentation might have occurred while membranes remained intact, as previously observed for *L. donovani* promastigotes treated with 4 mM H₂O₂ for 6 h [40]. We here showed that acidocalcisomes revealed by the pyrophosphatase immunolabeling were not significantly affected by eugenol concentrations. Nonetheless,

eugenol may still target Ca^{2+} . Indeed, an eugenol-rich *S. aromaticum* oil caused depolarization of the mitochondrial membrane [37], while an eugenol-rich essential oil from *Ocimum gratissimum* induced mitochondrial swelling after 72 h of treatment [41]. SQ109 is a drug inhibiting *Leishmania donovani* proliferation and was shown to cause deregulation of Ca^{2+} in mitochondria, via disruption of the mitochondrial membrane potential and acidocalcisomes, by their alkalinization [42]. These findings agree with the Alamar Blue assay results as cytochrome c oxidase is involved in mitochondrial energetic mechanisms.

This study also shows for the first time that eugenol dose-dependently decreases the concentration of intracellular lipid inclusions between 0.5 and $5 \times \text{IC}_{50}$. Miltefosine was shown to cause an overall depletion of lipid metabolites after 7.5 h of treatment, which was suggested to be caused by leakage and, thus, impairment of cellular membranes [43]. However, we observe a sharp decline in lipid droplets at concentrations for which membrane permeability and fluidity are not or very mildly affected. Lipids have a variety of functions in *Leishmania* sp. and some are linked to the structural needs of the parasites while others are linked to the metabolic needs as energy storage for the cells [36]. This could be due to the conversion and subsequent use of lipids to fulfill energetic needs in stress conditions induced by exposure to eugenol.

4. Materials and Methods

4.1. Chemicals and Reagents

Eugenol, amphotericin B, calcein, sephadex G-50, LH-20, ergosterol (Erg-), pentamidine isethionate, propidium iodide (PI), and 1,6-diphenyl-1,3,5-hexatriene (DPH) were obtained from Sigma-Aldrich (Bornem, Belgium). Miltefosine was obtained from Santa Cruz Biotechnology (Heidelberg, Germany). Calcein-AM included in a live/dead Viability/Cytotoxicity Kit for mammalian cells, Alamar blue and goat anti-Guinea Pig IgG Secondary Antibody, Alexa Fluor™ 488 were obtained from Thermo Fisher Scientific (Merelbeke, Belgium). The 1-palmitoyl-2-oleoyl-*sn*-glycero-3-phosphocholine (POPC), 1-palmitoyl-2-oleoyl-*sn*-glycero-3-phosphoethanolamine (POPE), L- α -phosphatidylinositol (PI—Liver, Bovine), and cholesterol (Chol—Ovine Wool) were purchased from Avanti Polar Lipids Inc. (Alabaster, AL, USA). All organic solvents used were from VWR (Leuven, Belgium).

4.2. Scanning Electron Microscopy

L. mexicana mexicana promastigotes at the density of 10^5 cells/mL were treated for 72 h with 0.5, 1, or $2 \times \text{IC}_{50}$ of eugenol ($\text{IC}_{50} = 16.59 \mu\text{M}$), or IC_{50} of amphotericin B ($\text{IC}_{50} = 0.25 \mu\text{M}$). After centrifugation at $600 \times g$ for 10 min, parasites were washed 2 times with phosphate-buffered saline (PBS, pH 7.4) and once with cacodylate buffer 0.1 M (pH 7.4). They were then immobilized on poly-L-lysine-coated coverslips for 5 min at room temperature. After washing 3 times with cacodylate 0.1 M (pH 7.4) to remove the excess of free-floating *Leishmania*, the coverslips were incubated in 1% glutaraldehyde in cacodylate 0.1 M (pH 7.4) to crosslink the fixed parasites on the poly-L-lysine coating. The parasites were postfixed with 1% osmium tetroxide in a cacodylate buffer for 2 h at 4 °C and washed in water to eliminate traces of the remaining osmium tetroxide, then dehydrated in a graded series of ethanol, critical-point dried, and coated with 10 nm of gold. Samples were observed with a CM12 Philips electron microscope at 80 kV.

4.3. Preparation of Large Unilamellar Vesicles (LUVs) Mimicking *Leishmania* Plasma Membrane

Based on the lipid profile of the isolated surface membrane of *L. donovani* promastigotes reported by Wassef et al. [44], LUVs composed of PC:PE:PI:Erg (10:26:12:15) were prepared using the extrusion technique with the Avanti Mini Extruder (Avanti Polar Lipids, Inc., Alabaster, AB, USA) [45]. Briefly, lipids were dissolved in chloroform to obtain a stock solution of 25 mg/mL and then mixed in the required ratio. The lipid film, which was formed after evaporating the solvent under a vacuum with a Buchi Rotavapor R-200, rotary evaporator (Büchi Labortechnik AG, Flawil, Switzerland), was hydrated by Tris 10 mM and NaCl 159 mM at pH 7.4. The suspension was submitted to five cycles of freezing–thawing to

obtain multilamellar vesicles (MLVs). The MLVs were extruded at 45 °C, 19 times through two polycarbonate Nucleopore Track Etch membrane filters (pore size = 100 nm) (Whatman Nucleopore, Corning Costar Corp., Badhoevedorp, The Netherlands) to obtain LUVs. Their size (average \pm 150 nm) and the polydispersity index (PDI < 0.2) were controlled via a dynamic light-scattering technique using Zetasizer Nano ZS (Malvern Instruments, Malvern, UK). The phospholipid content was measured by phosphorus assay [46] and then adjusted to a final concentration of 5 μ M.

To study the selective role of ergosterol, it was omitted in the preparation of some liposomes or replaced by cholesterol.

4.4. Calcein Release Assay

The leakage of calcein entrapped inside LUVs at the self-quenching concentration induced by a permeabilizing agent can be measured by fluorescence increase as calcein is diluted. For this permeability study, calcein, after purifying using column chromatography with sephadex LH-20, was diluted to the required concentration (73 mM) in the 10 mM Tris-HCl buffer solution at pH 7.4. This solution was then used for the hydration of the lipid film. The unencapsulated calcein was removed using the minicolumn centrifugation technique with sephadex G-50. Calcein-filled LUVs were incubated with eugenol or the reference drug amphotericin B, for 15 min at concentrations ranging from $0.5 \times IC_{50}$ to $40 \times IC_{50}$. Triton X 0.1% was used to induce 100% of the calcein leakage. After measuring the fluorescence intensity (excitation wavelength of 472 nm, emission wavelength of 512 nm) using a Perkin Elmer LS 30 Fluorescence Spectrophotometer (Perkin-Elmer Ltd., Beaconsfield, UK), the percentage of calcein released was calculated using the formula:

$$\% \text{ calcein release} = \frac{F_t - F_{ctrl}}{F_{tot} - F_{ctrl}} \times 100 \quad (1)$$

F_t : fluorescence signal measured in the presence of compound;

F_{ctrl} : fluorescence signal measured for LUVs control;

F_{tot} : fluorescence signal measured in the presence of Triton X-100;

Results are means of three independent experiments in triplicates.

4.5. DPH Fluorescence Anisotropy Assay

Fluorescence anisotropy values of DPH (r) can be used to probe the effect of a compound on membrane fluidity as the probe locates in the hydrophobic core of the lipid bilayer of the membrane and is sensitive to changes in the lipid acyl chain physical properties [47].

In LUVs- During the LUVs preparation process, DPH 2 mM in tetrahydrofuran was mixed with lipids at the molar ratio of 1:200 (DPH: lipid) before evaporating the solvents. The following steps were done as previously described in the section "Preparation of LUV mimicking *Leishmania* plasma membrane".

DPH-containing LUVs in a Tris HCl/NaCl buffer were then incubated with eugenol or amphotericin B for 30 min in the dark at the previously prepared concentrations. DPH was excited at 365 nm, and emission was read at 425 nm using an LS55 luminescence spectrometer connected to a circulating water bath to maintain the temperature at 28 °C [48].

DPH fluorescence anisotropy was determined using the equation:

$$r = \frac{I_{VV} - G \times I_{VH}}{I_{VV} + 2 \times G \times I_{VH}} \quad (2)$$

I_{VV} and I_{VH} : the fluorescence intensities with the excitation (wavelength of 365 nm) and emission (wavelength of 425 nm) polarization filters in vertical (v) and horizontal (h) orientations, respectively.

G: an inherent factor to the spectrophotometer used.

In *Lmm*- Samples were prepared as described by Xu et al. [49]. Briefly, parasites at the density of 10^7 cells/mL were treated for 24 h with eugenol (in the range of $1-40 \times IC_{50}$)

with IC_{50} 24 h = $5 \times IC_{50}$ 72 h, or reference drugs amphotericin B (in the range of $0.5\text{--}5 \times IC_{50}$) with IC_{50} 24 h = IC_{50} 72 h, and miltefosine (in the range of $1\text{--}10 \times IC_{50}$) with IC_{50} 24 h = $25.09 \mu\text{M} = 2 \times IC_{50}$ 72 h, then washed once with PBS, and resuspended in 1 mL of PBS. Then, 2 mM DPH in tetrahydrofuran were added to a final concentration of $0.5 \mu\text{M}$ and incubated in the dark for 20 min at 28°C (the concentration of tetrahydrofuran in *Leishmania* suspension was 0.025%).

DPH parameters are the same as previously described and Equation (2) was used to determine DPH anisotropy.

Results of the DPH anisotropy for both LUVs and *Lmm* are means of three independent experiments in triplicates.

4.6. Flow-Cytometry Analysis

Lmm promastigotes at the density of 10^7 cells/mL were treated for 8 h, 16 h, and 24 h with eugenol in the range of $1\text{--}40 \times IC_{50}$ (IC_{50} 8, 16 and 24 h = $5 \times IC_{50}$ 72 h), or by two reference drugs, amphotericin B in the range of $0.5\text{--}5 \times IC_{50}$ (IC_{50} 8, 16 and 24 h = IC_{50} 72 h), and miltefosine between 1 and $10 \times IC_{50}$ (IC_{50} 24 h = $2 \times IC_{50}$ 72 h). Treated parasites were collected by centrifugation at $600 \times g$ for 10 min. After washing once with PBS, *Lmm* promastigotes were resuspended in 1 mL of PBS-containing calcein-AM $0.1 \mu\text{M}$ and PI $3 \mu\text{M}$, then incubated for 15 min at room temperature in the dark. A total of 50,000 events per sample were acquired in a FACSCalibur cytometer using 488 nm excitation. Green fluorescence emission for calcein (530/30 bandpass) and red fluorescence emission for PI (610/20 bandpass) were measured.

4.7. Alamar Blue Assay

Using Alamar blue to analyze the effect of eugenol on the metabolic activity of *L. mexicana mexicana* promastigotes, parasites at the density of 10^7 cells/mL were incubated with eugenol, amphotericin B, or miltefosine at the same range of concentrations as the flow cytometry experiment. After 20 h of incubation at 28°C , Alamar blue (diluted 1:1 in PBS) was added and parasites were further incubated for 4 h at a final concentration of 4.5%. Fluorescence was measured on a spectrofluorimeter (SpectraMax-Molecular Devices, Berkshire, UK) (excitation wavelength of 530 nm, emission wavelength of 590 nm). The percentage of metabolic activity was calculated by comparing fluorescence values to those reported for the nontreated group.

4.8. Nile Red Labelling and Image Quantification

Lmm promastigotes at 10^7 cells/mL were treated for 24 h with eugenol at concentrations between 0.5 and $30 \times IC_{50}$ (IC_{50} 24 h = $5 \times IC_{50}$ 72 h). The parasites were then centrifuged at $600 \times g$ for 10 min. The pellet was washed twice with PBS 1X, then fixed in 4% PFA. Then, $10 \mu\text{L}$ of the sample were mixed with $30 \mu\text{L}$ of a $10 \mu\text{g/mL}$ Nile Red solution in acetone and incubated for 10 min. The mixture was observed in a Zeiss LSM980 microscope. Quantification of *Lmm* morphology was obtained by measuring 4–6 images from two independent experiments for the Feret maximum diameter (accounting for length) and the Feret minimum diameter (accounting for width). The Feret ratio of *Lmm* was then calculated as follows:

$$\text{Feret}_{\text{ratio}} = \frac{\text{Feret}_{\text{min}}}{\text{Feret}_{\text{max}}}$$

Similarly, quantification of the Nile Red fluorescence was done by measuring the mean green intensity in 4–6 images per concentration of eugenol after manually drawing the *Lmm* contour using confocal images in black and white. The results were obtained from 2 independent experiments.

4.9. Anti-TbVP1 Labelling and Image Quantification

Lmm promastigotes at the density of 10^7 cells/mL were treated for 24 h with eugenol at $1\text{--}30 \times IC_{50}$ (IC_{50} 24 h = $5 \times IC_{50}$ 72 h). Treated parasites were centrifuged at $600 \times g$ for

10 min. After washing twice with PBS, *Lmm* promastigotes were resuspended in 1 mL of PBS. Cells at 3×10^7 Lmm/mL were then transferred to a 24-well poly-l-lysine-coated plate. After several washes in PBS 1X, they were fixed with 4% formaldehyde in 0.1 M phosphate buffer for 20 min at room temperature. Permeabilization was done in 0.1% Triton-X100 for 5 min at room temperature. After several washes in Q-PBS (1% bovine serum albumin, lysine at 1 mg/mL, 0.01% saponin, and 0.025% azide in PBS 1X), the cells were incubated with anti-TbVP1 primary antibodies [50] for 1 h and then with fluorescent Alexa Fluor 488 goat antiguinea pig secondary antibodies for 1 h. The coverslips were mounted in prolong gold and left to polymerize for 24 h. The images were taken on a Zeiss LSM980 microscope. Quantification was obtained by measuring the mean green intensity of *Lmm* in 4–6 images per concentration of eugenol after manually drawing the *Lmm* contour using confocal images in black and white. The results were obtained from 1 experiment.

4.10. Statistical Analyses

All statistical tests were performed on GraphPad Prism 9.4.1. One-way ANOVA with Dunnett's post tests to compare the control versus compound-treated LUVs or *Leishmania* promastigotes, * $p < 0.05$; ** $p < 0.01$, *** $p < 0.001$, and **** $p < 0.0001$.

5. Conclusions

The results gave a better understanding of the processes involved in eugenol-mediated antileishmanial activity. Indeed, only the immunomodulatory effect of eugenol on mice with visceral leishmaniasis had been previously characterized. For the first time, it has here been demonstrated that eugenol, at concentrations close to its IC_{50} , lowers the metabolic activity of *Leishmania* promastigotes via a dose-dependent decrease of lipid droplets without impacting membrane integrity. Eugenol also induces morphological alterations, namely rounding and swelling of the promastigotes at such concentrations. Furthermore, eugenol has been demonstrated to not target membrane sterols, such as ergosterol, unlike amphotericin B. Further studies on the molecular targets of eugenol could prove interesting to propose its use in combination therapy with currently existing drugs.

Author Contributions: Conceptualization, J.Q.-L. and M.-P.M.-L.; methodology, D.T., M.-P.M.-L. and P.V.D.S.; formal analysis, K.H., P.V.D.S. and T.B.L.; investigation, K.H. and T.B.L.; writing—original draft preparation, K.H.; writing—review and editing, D.T., J.Q.-L., M.-P.M.-L. and P.V.D.S.; supervision, J.Q.-L. and M.-P.M.-L.; project administration, J.Q.-L.; funding acquisition, J.Q.-L. and M.-P.M.-L. All authors have read and agreed to the published version of the manuscript.

Funding: This work was supported by the Vietnamese Ministry of Education and Training (100/QĐ-BGDĐT), F.S.R-FNRS, T.0175.20, and by UCL (ARC 17.22.085).

Institutional Review Board Statement: Not applicable.

Informed Consent Statement: Not applicable.

Data Availability Statement: The data presented in this study are available in the manuscript.

Acknowledgments: The authors wish to thank Roberto Docampo for graciously providing anti-TbVP1 for our acidocalcisome experiments.

Conflicts of Interest: The authors declare no conflict of interest.

Sample Availability: Samples of the compounds are not available from the authors.

References

1. Centers for Disease Control and Prevention (CDC)—Leishmaniasis—Biology. Available online: <https://www.cdc.gov/parasites/leishmaniasis/biology.html> (accessed on 12 April 2022).
2. Ruiz-Postigo, J.A.; Jain, S.; Maia-Elkhoury, A.N.; Warusavithana, S.; Osman, M.; Lin, Z.; Beshah, A.; Yajima, A. Global Leishmaniasis Surveillance: 2019–2020, a Baseline for the 2030 Roadmap. *Wkly. Epidemiol. Rec.* **2021**, *96*, 401–419.
3. Kumari, D.; Perveen, S.; Sharma, R.; Singh, K. Advancement in Leishmaniasis Diagnosis and Therapeutics: An Update. *Eur. J. Pharmacol.* **2021**, *910*, 174436. [[CrossRef](#)] [[PubMed](#)]

4. Kumar Saha, A.; Mukherjee, T.; Bhaduri, A. Mechanism of Action of Amphotericin B on *Leishmania donovani* Promastigotes. *Mol. Biochem. Parasitol.* **1986**, *19*, 195–200. [[CrossRef](#)] [[PubMed](#)]
5. Ramos, H.; Saint-Pierre-Chazalet, M.; Bolard, J.; Cohen, B.E. Effect of Ketoconazole on Lethal Action of Amphotericin B on *Leishmania Mexicana* Promastigotes. *Antimicrob. Agents Chemother.* **1994**, *38*, 1079–1084. [[CrossRef](#)]
6. Shadab, M.; Jha, B.; Asad, M.; Deepthi, M.; Kamran, M.; Ali, N. Apoptosis-like Cell Death in *Leishmania donovani* Treated with KalsomeTM10, a New Liposomal Amphotericin B. *PLoS ONE* **2017**, *12*, e0171306. [[CrossRef](#)]
7. Machado, P.R.L.; Penna, G. Miltefosine and Cutaneous Leishmaniasis. *Curr. Opin. Infect. Dis.* **2012**, *25*, 141–144. [[CrossRef](#)]
8. Fernandes, K.S.; de Souza, P.E.N.; Dorta, M.L.; Alonso, A. The Cytotoxic Activity of Miltefosine against *Leishmania* and Macrophages Is Associated with Dynamic Changes in Plasma Membrane Proteins. *Biochim. Biophys. Acta (BBA)-Biomembr.* **2017**, *1859*, 1–9. [[CrossRef](#)]
9. Luque-Ortega, J.R.; Rivas, L. Miltefosine (Hexadecylphosphocholine) Inhibits Cytochrome c Oxidase in *Leishmania donovani* Promastigotes. *Antimicrob. Agents Chemother.* **2007**, *51*, 1327–1332. [[CrossRef](#)]
10. Moreira, R.A.; Mendanha, S.A.; Fernandes, K.S.; Matos, G.G.; Alonso, L.; Dorta, M.L.; Alonso, A. Miltefosine Increases Lipid and Protein Dynamics in *Leishmania Amazonensis* Membranes at Concentrations Similar to Those Needed for Cytotoxicity Activity. *Antimicrob. Agents Chemother.* **2014**, *58*, 3021–3028. [[CrossRef](#)]
11. Pinto-Martinez, A.K.; Rodriguez-Durán, J.; Serrano-Martin, X.; Hernandez-Rodriguez, V.; Benaim, G. Mechanism of Action of Miltefosine on *Leishmania donovani* Involves the Impairment of Acidocalcisome Function and the Activation of the Sphingosine-Dependent Plasma Membrane Ca²⁺ Channel. *Antimicrob. Agents Chemother.* **2017**, *62*, e01614-17. [[CrossRef](#)]
12. Mwenechanya, R.; Kovářová, J.; Dickens, N.J.; Mudaliar, M.; Herzyk, P.; Vincent, I.M.; Weidt, S.K.; Burgess, K.E.; Burchmore, R.J.S.; Pountain, A.W.; et al. Sterol 14 α -Demethylase Mutation Leads to Amphotericin B Resistance in *Leishmania mexicana*. *PLoS Negl. Trop. Dis.* **2017**, *11*, e0005649. [[CrossRef](#)]
13. Purkait, B.; Kumar, A.; Nandi, N.; Sardar, A.H.; Das, S.; Kumar, S.; Pandey, K.; Ravidas, V.; Kumar, M.; De, T.; et al. Mechanism of Amphotericin B Resistance in Clinical Isolates of *Leishmania donovani*. *Antimicrob. Agents Chemother.* **2012**, *56*, 1031–1041. [[CrossRef](#)]
14. Ponte-Sucre, A.; Gamarro, F.; Dujardin, J.-C.; Barrett, M.P.; López-Vélez, R.; García-Hernández, R.; Pountain, A.W.; Mwenechanya, R.; Papadopoulou, B. Drug Resistance and Treatment Failure in Leishmaniasis: A 21st Century Challenge. *PLoS Negl. Trop. Dis.* **2017**, *11*, e0006052. [[CrossRef](#)] [[PubMed](#)]
15. Mishra, J.; Singh, S. Miltefosine Resistance in *Leishmania donovani* Involves Suppression of Oxidative Stress-Induced Programmed Cell Death. *Exp. Parasitol.* **2013**, *135*, 397–406. [[CrossRef](#)] [[PubMed](#)]
16. Rijal, S.; Ostyn, B.; Uranw, S.; Rai, K.; Bhattarai, N.R.; Dorlo, T.P.C.; Beijnen, J.H.; Vanaerschot, M.; Decuypere, S.; Dhakal, S.S.; et al. Increasing Failure of Miltefosine in the Treatment of Kala-Azar in Nepal and the Potential Role of Parasite Drug Resistance, Reinfection, or Noncompliance. *Clin. Infect. Dis.* **2013**, *56*, 1530–1538. [[CrossRef](#)]
17. Islamuddin, M.; Chouhan, G.; Want, M.Y.; Ozbak, H.A.; Hemeg, H.A.; Afrin, F. Immunotherapeutic Potential of Eugenol Emulsion in Experimental Visceral Leishmaniasis. *PLoS Negl. Trop. Dis.* **2016**, *10*, e0005011. [[CrossRef](#)] [[PubMed](#)]
18. Le, T.B.; Beaufay, C.; Nghiem, D.T.; Mingeot-Leclercq, M.-P.; Quetin-Leclercq, J. In Vitro Anti-Leishmanial Activity of Essential Oils Extracted from Vietnamese Plants. *Molecules* **2017**, *22*, 1071. [[CrossRef](#)]
19. Milhaud, J.; Ponsinet, V.; Takashi, M.; Michels, B. Interactions of the Drug Amphotericin B with Phospholipid Membranes Containing or Not Ergosterol: New Insight into the Role of Ergosterol. *Biochim. Biophys. Acta (BBA)-Biomembr.* **2002**, *1558*, 95–108. [[CrossRef](#)]
20. Teerlink, T.; de Kruijff, B.; Demel, R.A. The Action of Pimaricin, Etruscomycin and Amphotericin B on Liposomes with Varying Sterol Content. *Biochim. Biophys. Acta (BBA)-Biomembr.* **1980**, *599*, 484–492. [[CrossRef](#)]
21. Kawato, S.; Kinoshita, K.; Ikegami, A. Dynamic Structure of Lipid Bilayers Studied by Nanosecond Fluorescence Techniques. *Biochemistry* **1977**, *16*, 2319–2324. [[CrossRef](#)] [[PubMed](#)]
22. Alonso, L.; Mendanha, S.A.; Dorta, M.L.; Alonso, A. Analysis of the Interactions of Amphotericin B with the *Leishmania* Plasma Membrane Using EPR Spectroscopy. *J. Phys. Chem. B.* **2020**, *124*, 10157–10165. [[CrossRef](#)] [[PubMed](#)]
23. Oliveira, I.H.R.; Figueiredo, H.C.P.; Rezende, C.P.; Verano-Braga, T.; Melo-Braga, M.N.; Reis Cunha, J.L.; de Andrade, H.M. Assessing the Composition of the Plasma Membrane of *Leishmania (Leishmania) infantum* and *L. (L.) amazonensis* Using Label-Free Proteomics. *Exp. Parasitol.* **2020**, *218*, 107964. [[CrossRef](#)] [[PubMed](#)]
24. Dos Santos, M.G.; Muxel, S.M.; Zampieri, R.A.; Pomorski, T.G.; Floeter-Winter, L.M. Transbilayer Dynamics of Phospholipids in the Plasma Membrane of the *Leishmania* Genus. *PLoS ONE* **2013**, *8*, e55604. [[CrossRef](#)] [[PubMed](#)]
25. Basmacıyan, L.; Azas, N.; Casanova, M. Calcein+/PI- as an Early Apoptotic Feature in *Leishmania*. *PLoS ONE* **2017**, *12*, e0187756. [[CrossRef](#)]
26. Basmacıyan, L.; Casanova, M. Cell Death in *Leishmania*. *Parasite* **2019**, *26*, 71. [[CrossRef](#)]
27. Khademvatan, S.; Gharavi, M.J.; Rahim, F.; Saki, J. Miltefosine-Induced Apoptotic Cell Death on *Leishmania major* and *L. Tropica* Strains. *Korean J. Parasitol.* **2011**, *49*, 17–23. [[CrossRef](#)]
28. De Jong, D.W.; Woodlief, W.G. Fluorimetric Assay of Tobacco Leaf Dehydrogenases with Resazurin. *Biochim. Biophys. Acta (BBA)-Enzymol.* **1977**, *484*, 249–259. [[CrossRef](#)]
29. O'Brien, J.; Wilson, I.; Orton, T.; Pognan, F. Investigation of the Alamar Blue (Resazurin) Fluorescent Dye for the Assessment of Mammalian Cell Cytotoxicity: Resazurin as a Cytotoxicity Assay. *Eur. J. Biochem.* **2000**, *267*, 5421–5426. [[CrossRef](#)]

30. Czekanska, E.M. Assessment of Cell Proliferation with Resazurin-Based Fluorescent Dye. In *Mammalian Cell Viability: Methods and Protocols*; Stoddart, M.J., Ed.; Methods in Molecular Biology; Humana Press: Totowa, NJ, USA, 2011; Volume 740, pp. 27–32, ISBN 978-1-61779-107-9.
31. Rampersad, S.N. Multiple Applications of Alamar Blue as an Indicator of Metabolic Function and Cellular Health in Cell Viability Bioassays. *Sensors* **2012**, *12*, 12347–12360. [[CrossRef](#)]
32. Barnes, S.; Spenny, J.G. Stoichiometry of the NADH-Oxidoreductase Reaction for Dehydrogenase Determinations. *Clin. Chim. Acta* **1980**, *107*, 149–154. [[CrossRef](#)]
33. Magnani, E.; Bettini, E. Resazurin Detection of Energy Metabolism Changes in Serum-Starved PC12 Cells and of Neuroprotective Agent Effect. *Brain Res. Protoc.* **2000**, *5*, 266–272. [[CrossRef](#)]
34. Duarte, M.; Ferreira, C.; Khandpur, G.K.; Flohr, T.; Zimmermann, J.; Castro, H.; Herrmann, J.M.; Morgan, B.; Tomás, A.M. Leishmania Type II Dehydrogenase Is Essential for Parasite Viability Irrespective of the Presence of an Active Complex I. *Proc. Natl. Acad. Sci. USA* **2021**, *118*, e2103803118. [[CrossRef](#)] [[PubMed](#)]
35. Patel, S.; Docampo, R. Acidic Calcium Stores Open for Business: Expanding the Potential for Intracellular Ca²⁺ Signaling. *Trends Cell. Biol.* **2010**, *20*, 277–286. [[CrossRef](#)] [[PubMed](#)]
36. Arya, R.; Dhembla, C.; Makde, R.D.; Sundd, M.; Kundu, S. An Overview of the Fatty Acid Biosynthesis in the Protozoan Parasite Leishmania and Its Relevance as a Drug Target against Leishmaniasis. *Mol. Biochem. Parasitol.* **2021**, *246*, 111416. [[CrossRef](#)] [[PubMed](#)]
37. Islamuddin, M.; Sahal, D.; Afrin, F. Apoptosis-like Death in *Leishmania donovani* Promastigotes Induced by Eugenol-Rich Oil of *Syzygium aromaticum*. *J. Med. Microbiol.* **2014**, *63*, 74–85. [[CrossRef](#)] [[PubMed](#)]
38. Darvishi, E.; Omid, M.; Bushehri, A.A.S.; Golshani, A.; Smith, M.L. The Antifungal Eugenol Perturbs Dual Aromatic and Branched-Chain Amino Acid Permeases in the Cytoplasmic Membrane of Yeast. *PLoS ONE* **2013**, *8*, e76028. [[CrossRef](#)] [[PubMed](#)]
39. Poojari, C.; Wilkosz, N.; Lira, R.B.; Dimova, R.; Jurkiewicz, P.; Petka, R.; Kepczynski, M.; Róg, T. Behavior of the DPH Fluorescence Probe in Membranes Perturbed by Drugs. *Chem. Phys. Lipids* **2019**, *223*, 104784. [[CrossRef](#)] [[PubMed](#)]
40. Das, M.; Mukherjee, S.B.; Shaha, C. Hydrogen Peroxide Induces Apoptosis-like Death in *Leishmania donovani* Promastigotes. *J. Cell Sci.* **2001**, *114*, 2461–2469. [[CrossRef](#)]
41. Ueda-Nakamura, T.; Mendonça-Filho, R.R.; Morgado-Díaz, J.A.; Korehisa Maza, P.; Prado Dias Filho, B.; Aparício Garcia Cortez, D.; Alviano, D.S.; Rosa, M.d.S.S.; Lopes, A.H.C.S.; Alviano, C.S.; et al. Antileishmanial Activity of Eugenol-Rich Essential Oil from *Ocimum gratissimum*. *Parasitol. Int.* **2006**, *55*, 99–105. [[CrossRef](#)]
42. Gil, Z.; Martínez-Sotillo, N.; Pinto-Martínez, A.; Mejías, F.; Martínez, J.C.; Galindo, I.; Oldfield, E.; Benaim, G. SQ109 Inhibits Proliferation of *Leishmania donovani* by Disruption of Intracellular Ca²⁺ Homeostasis, Collapsing the Mitochondrial Electrochemical Potential ($\Delta\psi_m$) and Affecting Acidocalcisomes. *Parasitol. Res.* **2020**, *119*, 649–657. [[CrossRef](#)]
43. Vincent, I.M.; Weidt, S.; Rivas, L.; Burgess, K.; Smith, T.K.; Ouellette, M. Untargeted Metabolomic Analysis of Miltefosine Action in *Leishmania infantum* Reveals Changes to the Internal Lipid Metabolism. *Int. J. Parasitol. Drugs Drug. Resist.* **2014**, *4*, 20–27. [[CrossRef](#)]
44. Wassef, M.K.; Fioretti, T.B.; Dwyer, D.M. Lipid Analyses of Isolated Surface Membranes of *Leishmania donovani* Promastigotes. *Lipids* **1985**, *20*, 108–115. [[CrossRef](#)] [[PubMed](#)]
45. Verstraeten, S.L.; Deleu, M.; Janikowska-Sagan, M.; Claereboudt, E.J.S.; Lins, L.; Tyteca, D.; Mingeot-Leclercq, M.-P. The Activity of the Saponin Ginsenoside Rh2 Is Enhanced by the Interaction with Membrane Sphingomyelin but Depressed by Cholesterol. *Sci. Rep.* **2019**, *9*, 7285. [[CrossRef](#)] [[PubMed](#)]
46. Bartlett, G.R. Phosphorus Assay in Column Chromatography. *J. Biol. Chem.* **1959**, *234*, 466–468. [[CrossRef](#)] [[PubMed](#)]
47. do Canto, A.M.T.M.; Robalo, J.R.; Santos, P.D.; Carvalho, A.J.P.; Ramalho, J.P.P.; Loura, L.M.S. Diphenylhexatriene Membrane Probes DPH and TMA-DPH: A Comparative Molecular Dynamics Simulation Study. *Biochim. Biophys. Acta (BBA)-Biomembr.* **2016**, *1858*, 2647–2661. [[CrossRef](#)] [[PubMed](#)]
48. Deleu, M.; Lorent, J.; Lins, L.; Bresseur, R.; Braun, N.; El Kirat, K.; Nylander, T.; Dufrêne, Y.F.; Mingeot-Leclercq, M.-P. Effects of Surfactin on Membrane Models Displaying Lipid Phase Separation. *Biochim. Biophys. Acta* **2013**, *1828*, 801–815. [[CrossRef](#)] [[PubMed](#)]
49. Xu, W.; Hsu, F.-F.; Baykal, E.; Huang, J.; Zhang, K. Sterol Biosynthesis Is Required for Heat Resistance but Not Extracellular Survival in *Leishmania*. *PLoS Pathog.* **2014**, *10*, e1004427. [[CrossRef](#)]
50. Lemercier, G.; Dutoya, S.; Luo, S.; Ruiz, F.A.; Rodrigues, C.O.; Baltz, T.; Docampo, R.; Bakalara, N. A Vacuolar-Type H⁺-Pyrophosphatase Governs Maintenance of Functional Acidocalcisomes and Growth of the Insect and Mammalian Forms of *Trypanosoma brucei*. *J. Biol. Chem.* **2002**, *277*, 37369–37376. [[CrossRef](#)]

Disclaimer/Publisher's Note: The statements, opinions and data contained in all publications are solely those of the individual author(s) and contributor(s) and not of MDPI and/or the editor(s). MDPI and/or the editor(s) disclaim responsibility for any injury to people or property resulting from any ideas, methods, instructions or products referred to in the content.